# NATIONAL ADVISORY COMMITTEE FOR AERONAUTICS

**TECHNICAL NOTE 3622**

## PRELIMINARY STUDY OF SOME FACTORS WHICH AFFECT THE STALL-FLUTTER CHARACTERISTICS OF THIN WINGS

By A. Gerald Rainey

Langley Aeronautical Laboratory
Langley Field, Va.


Washington
March 1956

Z

NATIONAL ADVISORY COMMITTEE FOR AERONAUTICS

TECHNICAL NOTE 3622

# PRELIMINARY STUDY OF SOME FACTORS WHICH AFFECT THE STALL-FLUTTER CHARACTERISTICS OF THIN WINGS[1]

By A. Gerald Rainey

## SUMMARY

The results of an exploratory, analytical, and experimental study of some of the factors which might be of importance in the stall flutter of thin wings are presented. The factors considered were Mach number, Reynolds number, density, aspect ratio, sweepback, structural damping, location of torsion nodal line, and concentrated tip weights.

The importance of aerodynamic torsional damping in the stall flutter of thin wings has been demonstrated through comparison of regions of negative torsional damping and regions of flutter.

The results of a series of experiments on a thin wing tested at various lengths indicate that compressibility definitely alters the stall-flutter characteristics of wings of this type and that the compressibility effects appear to depend on the aspect ratio.

A brief study of the inertia effects of concentrated tip weights indicates that such effects can be important; however, the large number of parameters involved makes it difficult to generalize the results. An approximate analysis is presented for obtaining an estimate of the stall-flutter characteristics of particular wing-weight configurations.

Some of the other factors considered were found to be more or less significant; however, all the factors will require further study if their effects are to be more fully interpreted.

## INTRODUCTION

In general, as the angle of attack of a wing is increased to values near the angle of stall, the flutter velocity is decreased to values much lower than that observed at angles near zero lift. Since the potential-flow theories of classical flutter do not indicate an effect

[1]Supersedes recently declassified NACA Research Memorandum L52D08 by A. Gerald Rainey, 1952.

of lift coefficient, the decrease in flutter velocity is presumed to be associated with nonpotential flow and has come to be known as stall flutter even though the wing may not be completely stalled in the usual sense of the word. Near zero lift the type of flutter which occurs is usually a coupled, bending-torsion type, whereas flutter encountered at the higher angles of attack is usually predominantly a single-degree-of-freedom flutter occurring in the torsional mode.

Much information exists concerning the stall flutter of moderately thick wings at low speeds (refs. 1 to 6) and the effects of several parameters on the stall flutter of thin propeller blades have been presented in reference 7. While stall flutter has not been considered a serious problem in the design of conventional wings (previous to 1950), experience with thin propeller blades indicates that stall flutter may become an important consideration in the design of thin wings. Since designers are considering the use of thin wings for high-speed airplanes, it was considered desirable to reexamine the stall-flutter problem.

The purpose of this paper is to present the results of an exploratory, analytical, and experimental study of some of the factors which might be of importance in the stall flutter of thin wings. The factors considered are Mach number, Reynolds number, density, aspect ratio, sweepback, structural damping, location of torsion nodal line, and concentrated tip weights. The results obtained by variation of any particular parameter are somewhat sketchy since the purpose of this investigation is to search for the significant parameters rather than to define completely the effect of the significant parameters.

## SYMBOLS

| | |
|---|---|
| $a$ | speed of sound, ft/sec |
| $a_o$ | initial amplitude of oscillation, radians |
| $a_n$ | amplitude of oscillation after $n$ cycles, radians |
| $b$ | semichord perpendicular to leading edge, ft |
| $C_\alpha$ | torsion spring constant per unit span, ft-lb/ft-radian |
| $c$ | chord, ft $(2b)$ |
| $\frac{dE}{dt}$ | time derivative of energy, ft-lb/sec |

| | |
|---|---|
| $f_\alpha(x)$ | spanwise torsional deflection function |
| $f_{h_1}$ | first natural bending frequency, cps |
| $f_{\alpha_1}$ | first natural torsion frequency, cps |
| $f_{exp}$ | experimental flutter frequency, cps |
| $g$ | damping coefficient |
| $g_\alpha$ | structural damping coefficient for torsion mode |
| $I_\alpha$ | moment of inertia per unit span about the elastic axis, slug-ft$^2$/ft |
| $K_\alpha$ | spring constant of damping apparatus, ft-lb/radian |
| L | wing length, ft |
| M | twisting moment per unit span, ft-lb/ft |
| $M_a$ | complex aerodynamic moment per unit span per radian deflection ft-lb/ft-radian |
| $M_{\dot{\alpha}}$ | aerodynamic moment per radian in phase with velocity, ft-lb/radian |
| $m_{\dot{\alpha}}$ | coefficient of aerodynamic moment per radian in phase with velocity |
| n | number of cycles |
| $\left(\frac{r_\alpha^2}{\kappa}\right)_e$ | effective inertia parameter where $r_\alpha$ is the effective radius of gyration and $\kappa$ is the effective mass density ratio |
| R | Reynolds number |
| S | wing area, ft$^2$ |
| V | velocity, ft/sec |
| x | distance along span, ft |
| $\alpha$ | angular deflection, radians |

| | |
|---|---|
| $\dot{\alpha}$ | angular velocity, radians/sec |
| $\ddot{\alpha}$ | angular acceleration, radians/sec$^2$ |
| $\alpha_i$ | angle of attack at root, degrees |
| $\alpha_o$ | amplitude of torsional oscillation, radians |
| $\Lambda$ | angle of sweepback, degrees |
| $\rho$ | density of test medium, slugs/ft$^3$ |
| $\omega$ | frequency of oscillation, radians/sec |
| $\omega_\alpha$ | first natural torsional frequency, radians/sec $\left(\omega_\alpha = 2\pi f_{\alpha_1}\right)$ |

## METHODS AND APPARATUS

The experimental investigation consisted of essentially two phases: (1) conventional flutter tests with the addition of the angle of attack as a primary variable and (2) aerodynamic damping measurements with the angle of attack again being a primary variable.

### Wind Tunnel

The experiments were conducted in the Langley 4.5-foot flutter research tunnel which is of the closed-throat single-return type employing both air and Freon 12 as a testing medium at pressures from one atmosphere down to 1/8 atmosphere. During the course of this investigation the test section of the 4.5-foot-diameter flutter tunnel was altered to a rectangular section 2 feet by 4 feet to accommodate other types of investigations. The effects of this change in test section have not been evaluated but they are believed to be small.

### Models

Five thin wings were used for the experiments and are illustrated in figure 1. Wing number 1 was originally 24 inches long; however, in order to investigate the effects of aspect ratio, this wing was shortened in steps of three inches and the various configurations are designated wing number 1-24, 1-21, 1-18, and so forth. When equipped with a tip weight the wing designation is followed by the letter W, such as 1-21W. The model designations, properties, and test conditions are listed in table I.

Wing number 1 was of solid aluminum-alloy construction and was used in studying the effects of Mach number, aspect ratio, and concentrated weights on stall flutter. This wing also was used to measure the aerodynamic damping moment for torsional oscillations. A series of four wings (designated 2, 3, 4, and 5) varying in sweep angle and aspect ratio were employed to study the stall-flutter characteristics of swept wings. These wings were constructed of wood laminations on a stainless steel plate and the length-to-chord ratio was kept constant at 2.7.

Each of the five wings was equipped with resistance-wire strain gages arranged to obtain a record of the flutter frequency and to indicate the relative magnitude of the strains in the bending and torsion degrees of freedom at flutter.

## Flutter Tests

During the flutter tests the models were mounted as cantilever beams on a heavy, rigid mount which could be rotated and clamped at any desired angle of attack. With the wing clamped at the desired angle of attack, the airspeed of the tunnel was slowly increased until a steady or divergent oscillation of the model occurred. At this point the tunnel conditions were observed and an oscillographic record of the strain-gage outputs was obtained. The velocity at this point was considered to be the minimum flutter velocity for the wing tested at that particular angle of attack. In some cases the amplitudes encountered at this velocity were sufficiently mild so that the velocity could be increased further until some limiting condition was reached, such as excessive vibration amplitudes, excessive static bending load, or maximum tunnel velocity. The same procedure was then repeated for angle-of-attack increments of $2^\circ$ or less at various angles throughout the range from $0^\circ$ to $24^\circ$.

The effects of density, Reynolds number, and Mach number were studied by performing the above experiments at various pressures from atmospheric down to 1/8 atmosphere in both air and Freon 12.

The effects of aspect ratio and Mach number were investigated by shortening wing number 1 in steps of three inches.

The effects of concentrated tip weights were studied, briefly, by clamping a solid ellipsoid, cast of an alloy of bismuth, tin, and lead, 10 inches long and 0.75 inch in diameter to the tip of wings number 1-21 and 1-18. The center of gravity of the weight was placed at the 50-percent-chord line, 0.375 inch inboard from the tip in the plane of the wing. The characteristics of the wings equipped with the weight are listed in table I under the designations 1-21W and 1-18W.

## Aerodynamic Damping Measurements

The aerodynamic torsional damping moment was measured by the method of decaying oscillations (ref. 8).

A special wing mount (shown schematically in fig. 2) was designed and built for wing number 1-24 to allow torsional oscillations but restrict the bending mode. The root of the wing was restrained in torsion only by two relatively soft coil springs. The first natural torsional frequency of the wing-shaft-spring system was about 1/8 of the first natural torsional frequency of wing number 1-24 when mounted as a cantilever. In the special mount the wing tip was restrained in bending by a steel cable and, consequently, the first natural bending frequency of the wing in the damping mount was appreciably higher than in the cantilever condition. For these reasons the wing was considered as a rigid body (constant angle of attack spanwise) when oscillating at the first natural torsional frequency of the wing-shaft-spring system.

The damping of the system was obtained by deflecting the wing-shaft-spring system in torsion to an amplitude of approximately $3^\circ$ from the mean angle of attack. The wing was then released and the resulting oscillation was recorded. The damping coefficient was computed from the following relationship (ref. 9):

$$g = \frac{1}{\pi n} \log_e \frac{a_o}{a_n}$$

and the aerodynamic damping moment was computed from

$$M_{\dot{\alpha}} = \left(g_{total} - g_{tare}\right)K_\alpha = g_{aero}K_\alpha$$

where $g_{total}$ is the damping coefficient obtained with air flow and $g_{tare}$ is the damping coefficient obtained with no air flow. The nondimensional aerodynamic damping moment coefficient is defined as

$$m_{\dot{\alpha}} = \frac{M_{\dot{\alpha}}}{\frac{\rho}{2}V^2Sc}$$

The aerodynamic torsional damping moment coefficient was obtained at various angles of attack by rotation of the entire wing-shaft-spring system to the desired angle of attack. The coefficient was determined as a function of $V/b\omega$ for angles of attack of $0^\circ$, $4^\circ$, $8^\circ$, $12^\circ$, $16^\circ$, and $20^\circ$.

The effects of the location of the axis of rotation or torsion nodal line were studied by clamping the wing to the shaft so that the axis of the shaft coincided with the desired chordwise location. The nodal line positions studied were 25, 32.5, 50, and 75 percent of the chord rearward of the leading edge.

The maximum Mach number reached in the damping measurements was about 0.2; the maximum Reynolds number was about $0.8 \times 10^6$.

## RESULTS AND DISCUSSION

### General Remarks Concerning the Effects of Lift Coefficient on the Flutter of Wings

In general, it has been found that as the angle of maximum lift is approached the flutter velocity is reduced appreciably from the value obtained at angles near zero lift. In addition, the mode of flutter at the higher angles of attack is usually predominantly a single-degree-of-freedom flutter occurring in the torsional mode. Since this type of flutter is associated with nonpotential flow, the phenomenon, as previously noted, has come to be known as stall flutter.

A typical low Mach number variation of the flutter velocity coefficient with angle of attack for thin wings is shown in figure 3. The flutter velocity is plotted in the nondimensional form $V/b\omega_\alpha$ as a function of the angle of attack at the root for wing number 2. The lower boundary in figure 3 represents the velocity at which an oscillation first started. The upper curve from $\alpha_i = 6^\circ$ to $\alpha_i = 18^\circ$ represents the velocity at which the oscillation reached dangerous amplitudes. The area labeled "flutter free" between $20^\circ$ and $24^\circ$ is bounded by the velocity coefficients at which the oscillation stopped. In this range of angle of attack the velocity was increased until the static bending load on the wing became excessive. The limiting velocity is indicated by the upper dashed curve.

As the angle of attack is increased the flutter velocity coefficient decreases rapidly and reaches a minimum value near $\alpha_i = 16^\circ$. The flutter velocity coefficient $V/b\omega_\alpha$ at this minimum point is approximately equal to 1.0. The velocities listed in table I correspond to this minimum value for the various configurations and test conditions shown. Experimental evidence obtained on numerous propeller blades in reference 7 and on several thin wings in the present investigation indicates that the "rule-of-thumb," $V/b\omega_\alpha \cong 1.0$, for estimating the minimum flutter velocity of simple thin wings may be quite useful. Of course, the exceptions to this elementary rule are numerous as will be indicated in the subsequent discussion of the various factors studied.

The remainder of the data shown in figure 3, other than the minimum point, do not lend themselves to generalities other than, perhaps, a few speculative remarks regarding the possible causes of the flutter. At zero angle of attack the flutter was a coupled bending-torsion type and the flutter frequency was at some value between the natural first bending frequency and the natural first torsional frequency. As the angle of attack was increased, the flutter-velocity coefficient decreased rapidly and the flutter frequency gradually approached the torsional frequency. This decrease in flutter velocity is probably due to a decrease in aerodynamic damping resulting from partial separation and boundary-layer time-lag effects. McCullough and Gault in reference 10 indicate that, for steady flow, relatively sharp-edged airfoils exhibit a measurable region of separated flow near the leading edge at angles of attack as low as $\alpha = 1^{\circ}$. As the angle of attack is increased this separated-flow region is extended and, presumably, the boundary-layer time-lag effects become more pronounced. The mechanism of this decrease in damping is not clearly understood and would be difficult to treat analytically.

As the angle of attack is increased to values well beyond the steady-state stall angle ($\alpha_i \cong 20^{\circ}$ to $24^{\circ}$), the vibration encountered resembles a forced vibration rather than a self-excited vibration. The amplitude of vibration increased gradually as the velocity was increased beyond the initial vibration point then, after reaching a maximum value, decreased to zero at the velocities indicated in figure 3. In this region of angle of attack, the vortex frequency, estimated on the basis of the projected wing area, was of the same order as the vibration frequency which was within a few percent of the natural torsional frequency. Although the motion under these conditions closely resembles a forced oscillation, it is difficult to separate the phenomenon at very high angles from the phenomenon at moderate angles and for that reason the oscillations at all angles of attack will be referred to as flutter.

## Some Considerations of Aerodynamic Damping

As long ago as 1928 Frazer and Duncan (ref. 1) hypothesized that the decrease in flutter speed with increasing angle of attack may be accounted for by a decrease of the aerodynamic torsional damping. In 1943 Mary Victory (ref. 5) used a conventional flutter analysis altering only the torsional damping coefficients to calculate with good agreement several stall-flutter conditions obtained experimentally by Studer (ref. 2). The damping coefficients used in Victory's analysis were obtained experimentally on a similar wing at about the same values of Reynolds number and frequency as the flutter data of Studer.

Some of the aerodynamic torsional damping coefficients measured using wing number 1-24 are shown in figure 4(a). Contours of constant

values of the coefficient are shown in figure 4(a) as functions of $V/b\omega$ and angle of attack with the axis of rotation at the midchord. The curves above the zero damping line represent increasing values of negative damping, except at the higher angles of attack where the damping decreased to zero then became positive again at higher values of $V/b\omega$. The area enclosed by the zero damping curves represents a region where a single-degree-of-freedom torsional instability is possible.

For comparison, the actual flutter regions obtained for the same wing (no. 1-24) while mounted as a cantilever are shown in figure 4(b). One interesting feature of these data lies in the similarity of the flutter regions of figure 4(b) to the regions of negative damping shown in figure 4(a). This similarity is rather striking when it is realized that the damping data were obtained when the wing was mounted in a mechanism which provided appreciably different boundary conditions from those provided by the simple cantilever mount. The frequency of the wing mounted in the damping mechanism was about one-eighth of the torsional frequency of the wing mounted as a cantilever. The damping mechanism severely restricted the bending degree of freedom, whereas the cantilever mount, of course, allowed this degree of freedom. The maximum Mach number of the damping measurements was about 0.2 as compared with a Mach number of about 0.75 for the flutter tests. The dissimilarity between the two sets of data at the lower angles of attack is attributed to compressibility effects which will be discussed later. In view of the similarity of the regions which occurred in spite of the widely different conditions which applied to the two determinations, it appears that the torsional aerodynamic damping is very important in the stall flutter of thin wings.

## Stall-Flutter Analysis

The problem of calculating stall-flutter velocities has been a subject of much interest and some of the more promising approaches are discussed in reference 6. At the present time, no satisfactory stall-flutter analysis has been developed. This lack of an adequate analytical approach is due, primarily, to the difficulty in treating the air forces. The problem is somewhat similar to that of predicting the maximum lift coefficient. Presumably, if the oscillatory air forces were known for the proper range of significant variables, the analysis of stall flutter would be relatively simple. Unfortunately, the large number of significant variables makes it impractical to obtain adequate air-force coefficients except over very limited ranges.

Observations of the stall-flutter characteristics of the unswept wings used in the present investigation indicate the possibility of applying a relatively simple analysis employing the measured aerodynamic torsional damping coefficients. The observations are: (1) The flutter

occurs in almost a pure torsional mode with very little translation of the elastic axis and (2) the flutter frequency is very nearly equal to the first natural torsional frequency. (See table I.) Based on these observations a simplified single-degree-of-freedom analysis (developed in the appendix) yields the following relation:

$$g_\alpha\left(\frac{r_\alpha^2}{\kappa}\right)_e + \frac{2m_{\dot{\alpha}}}{\pi}\left(\frac{V}{b\omega_\alpha}\right)^2 = 0$$

Since the structural damping is always positive, at flutter the aerodynamic torsional damping must be negative and at least equal to the structural torsional damping.

If the aerodynamic torsional damping moment coefficients are available for the proper range of significant variables, the flutter velocity can be calculated. The aerodynamic damping moment coefficients measured in the present investigation are presented in figure 5 for the various angles of attack and axes of rotation. The figure shows the values of the quantity $\frac{2m_{\dot{\alpha}}}{\pi}\left(\frac{V}{b\omega_\alpha}\right)^2$ (the form most convenient for the calculations) as functions of $V/b\omega$. For a given wing the quantity

$$g_\alpha\left(\frac{r_\alpha^2}{\kappa}\right)_e = g_\alpha \frac{\int_0^L I_\alpha \left[f_\alpha(x)\right]^2 dx}{\int_0^L \pi\rho b^4 \left[f_\alpha(x)\right]^2 dx}$$

may be estimated, calculated, or measured, and the flutter velocity may be determined from the figures at each angle of attack where the aerodynamic damping is negative. Of course, at the lower angles of attack where the flutter can no longer be represented as a single-degree-of-freedom torsional vibration, the analysis is meaningless.

Effects of structural damping.- One of the parameters which can cause deviations from the "rule of thumb" mentioned previously, that is, $(V/b\omega_\alpha)_{min} \cong 1.0$, is the structural damping coefficient $g_\alpha$. This effect of structural damping (based on the preceding analysis) is illustrated in figure 6 where the minimum flutter velocity is shown as a function of the effective inertia parameter for several values of structural damping. The analytical results shown are for the axis of rotation at the midchord. The horizontal line for zero structural

damping indicates that the minimum flutter-velocity coefficient would be independent of the inertia parameter for this hypothetical condition. The addition of a small amount of damping increases the minimum flutter velocity coefficient appreciably and makes the coefficient a function of $\left(\frac{r_\alpha^2}{\kappa}\right)_e$. A thin solid aluminum-alloy wing at sea-level density would have a value of $\left(\frac{r_\alpha^2}{\kappa}\right)_e$ near 20. Increasing the structural damping coefficient from 0.001 to 0.010 would approximately double the minimum flutter velocity coefficient.

Effects of fluid density.- Variation of the density can cause deviations from the nominal minimum flutter velocity coefficient of 1.0. This effect is illustrated in figure 7, where the minimum flutter velocity coefficient is plotted as a function of the quantity $g_\alpha\left(\frac{r_\alpha^2}{\kappa}\right)_e$ which is inversely proportional to density. The solid curve, which was calculated for the midchord axis of rotation by the analysis previously discussed, rises sharply at values of $g_\alpha\left(\frac{r_\alpha^2}{\kappa}\right)_e$ representing high density then tends to level off at values corresponding to reduced density. The hypothetical thin aluminum-alloy wing mentioned earlier would have a value of $g_\alpha\left(\frac{r_\alpha^2}{\kappa}\right)_e$ of about 0.02 for a damping coefficient of $g_\alpha = 0.001$ at sea level. The analysis indicates that the minimum flutter velocity coefficient would be increased from about 0.8 at sea level to 1.2 by decreasing the density to that at 40,000 feet altitude.

Effects of location of the axis of rotation.- The effects of the location of the axis of rotation can be estimated with the aid of the aerodynamic torsional damping coefficients for various axes of rotation. Examination of figure 5 indicates a definite reduction in the extent of the negative damping regions for the forward locations of the axis of rotation. It appears, therefore, that the stall-flutter problem for wings having a torsion nodal line well forward may be greatly relieved as compared with the problem for wings having rearward locations of the torsion nodal line.

## Effects of Reynolds Number

The effects of Reynolds number on stall flutter have not been thoroughly investigated; however, a few speculative remarks are possible. At low Mach numbers the aerodynamic characteristics of thin unswept wings

at high angles of attack are relatively insensitive to changes in Reynolds number. For this reason, it seems that Reynolds number might be relatively unimportant in the stall flutter of thin unswept wings at low Mach numbers. This supposition is at least partially verified by some of the data shown in figure 7, which shows that the minimum flutter-speed coefficient for wing number 1-24 increased from $\frac{V}{b\omega_\alpha} = 0.750$ to $\frac{V}{b\omega_\alpha} = 0.846$ over a range of density. The corresponding range of Reynolds number was from $3.41 \times 10^6$ to $0.085 \times 10^6$. The increase in flutter velocity coefficient with decreased density is in qualitative agreement with the trend predicted by the analysis.

The effects of Reynolds number at high Mach numbers and for swept wings are appreciably more obscure and require further investigation.

## Effects of Mach Number and Aspect Ratio on the Stall Flutter of Unswept Wings

The "rule-of-thumb" mentioned earlier, that is, $\left(\frac{V}{b\omega_\alpha}\right)_{min} \cong 1.0$ or $(V)_{min} \cong b\omega_\alpha$, could be used to predict the minimum Mach number at which flutter might occur if compressibility did not alter this minimum flutter velocity coefficient. The minimum flutter Mach number $(V/a)_{min}$ would simply be $b\omega_\alpha/a$; however, Baker (ref. 7) found that, for thin propeller blades, $(V/b\omega_\alpha)_{min}$ was a function of Mach number. By varying the speed of sound a, it was shown that the minimum flutter Mach number became a nonlinear function of $b\omega_\alpha/a$ at the higher Mach numbers, and at sufficiently high values of $b\omega_\alpha/a$ (approx. 0.5) no flutter occurred up to the limit of the tests $\left(M_{tip} = 1.4\right)$.

The results of the present investigation of compressibility effects are shown in figure 8. The minimum flutter Mach number is shown as a function of the quantity $b\omega_\alpha/a$ for wings number 1-24 to 1-15. Since it was not possible to obtain a sufficiently wide variation of $b\omega_\alpha/a$ by varying the speed of sound, it was necessary to increase $\omega_\alpha$ by reducing the length of the original wing number 1-24. Consequently, the effects obtained may be thought of as combined effects of Mach number and aspect ratio. The results obtained on wing number 1-24 show a fairly linear relationship between the minimum flutter Mach number and $b\omega_\alpha/a$ and give no indication of an approaching limiting value of $b\omega_\alpha/a$ beyond which flutter would not occur. The value of $b\omega_\alpha/a$ reached in these tests was about 0.43, which is slightly less than the value of 0.5 presented in reference 7 as the value required to eliminate stall flutter of propeller blades. Wing number 1-21 was tested at values

of $b\omega_\alpha/a$ up to 0.5 and, although flutter was not eliminated at any value of $b\omega_\alpha/a$, the shape of the curve of minimum flutter Mach number as a function of $b\omega_\alpha/a$ (shown in fig. 8) indicated that a limiting value was approached at $\frac{b\omega_\alpha}{a} = 0.5$. With wing number 1-18 a new curve was defined with an apparent limiting value somewhere near $\frac{b\omega_\alpha}{a} = 0.59$. When wing number 1-15 was tested at $\frac{b\omega_\alpha}{a} = 0.7$, no flutter was obtained up to the choking Mach number of the tunnel ($M \cong 0.8$); however, intermittent flutter did occur at $\frac{b\omega_\alpha}{a} = 0.67$, indicating that a more nearly complete curve for this wing might have a shape similar to the dashed curve shown.

The results of this series of experiments on one thin wing at various lengths indicate that compressibility definitely alters the stall-flutter characteristics of wings of this type. Furthermore, the compressibility effects appear to depend, to a large extent, on the aspect ratio.

## Effects of Sweepback

The available data on the effects of sweepback on stall flutter of thin wings are limited to a series of experiments on wings number 2, 3, 4, and 5. In figure 9 the variation of the flutter velocity coefficient with angle of attack at atmospheric pressure is presented for the four wings varying in angle of sweepback from 0° to 45°.

The curves for the 0°, 15°, and 30° wings are very similar, indicating no significant effect of sweep angle up to 30° for this series of wings. The 45° swept wing, however, did not experience flutter at high angles of attack even though the velocity was increased to about 80 percent of the flutter velocity obtained at zero angle of attack. The tests on the 45° wing were stopped at conditions indicated by the dashed curve because of the excessive static bending load on the wing.

The results of the present experiments indicate the possible importance of sweepback; however, additional research will be required before the sweepback effects can be applied to other configurations and test conditions.

## Inertia Effects of Concentrated Tip Weights

The inertia effects of concentrated tip weights on the stall-flutter characteristics of thin wings were investigated by equipping wings number 1-21 and 1-18 with a dense ellipsoid. High-density material was used to obtain a small volume so that the aerodynamic effects of the mass would be a minimum. The aerodynamic effects of large bodies on stall flutter have not been investigated. The weight reduced the natural torsional frequency of both wings approximately by a factor of 0.5.

The variation of the flutter velocity coefficient with angle of attack for wings number 1-21 and 1-18 both with and without the weight is shown in figure 10. When tested without the weight both wings had a minimum flutter velocity coefficient of about 1.0, and this minimum occurred between $\alpha_i = 16^\circ$ and $\alpha_i = 20^\circ$. When tested with the weight, the minimum flutter velocity coefficient was increased to about 3.0 and the angle of attack at which this minimum occurred was decreased to about $\alpha_i = 8^\circ$ or $10^\circ$. For comparison, the calculated variation (see section entitled "Stall-Flutter Analysis") for both wings with and without the weight are shown in the same figure. The calculated results show the same trend as the experimental results in that the calculations indicate a large increase in the minimum flutter velocity coefficient and a decrease of the angle of attack at which this minimum occurs when the wing is equipped with a weight.

The results shown in figure 10 indicate that the minimum flutter velocity coefficient for these two wings was approximately tripled by equipping the wings with a concentrated tip weight, and the minimum flutter velocity was approximately doubled. It should not be concluded, however, that the addition of a weight always increases the minimum flutter velocity. The analysis on which the calculated results are based indicates that the minimum flutter velocity for a thin unswept wing at low Mach numbers depends on the amount and distribution of mass or inertia, the fluid density, and the structural damping. For example, when wing number 1-18W was tested in Freon (high density) the minimum flutter velocity coefficient was about 1.5 as compared with 1.0 for wing number 1-18. The actual velocity, however, was a few percent lower for the weighted condition.

Because of the many variables of importance in the stall flutter of wings with concentrated tip weights, it is not possible to generalize the results of this brief investigation. The inertia effects of a particular wing-weight configuration can be estimated by use of figure 7 where the minimum flutter velocity coefficient is shown as a function of the quantity $g_\alpha\left(\frac{r_\alpha^2}{\kappa}\right)_e$. The symbols represent experimentally

determined values for several wing-weight-density combinations and the solid curve represents calculated minimum values for wings having a torsion nodal line near the midchord. The analysis agrees qualitatively with the experiments.

## CONCLUDING REMARKS

The importance of aerodynamic torsional damping in the stall flutter of thin wings has been demonstrated through comparison of regions of negative torsional damping and regions of flutter.

The results of a series of experiments on a thin wing tested at various lengths indicate that compressibility definitely alters the stall-flutter characteristics of wings of this type and that the compressibility effects appear to depend on the aspect ratio.

A brief study of the inertia effects of concentrated tip weights indicates that such effects can be important; however, the large number of parameters involved makes it difficult to generalize the results. An approximate analysis is presented for obtaining an estimate of the stall-flutter characteristics of particular wing-weight configurations.

Some of the other factors considered (Reynolds number, sweepback, fluid density, structural damping, and location of torsion nodal line) were found to be more or less significant; however, all the factors would require further study if their effects are to be more fully interpreted.

Langley Aeronautical Laboratory
National Advisory Committee for Aeronautics
Langley Field, Va., March 31, 1952.

## APPENDIX

A simplified single-degree-of-freedom-flutter analysis using experimentally determined aerodynamic damping coefficients has been developed in order to provide some means for estimation of stall-flutter velocities of thin wings.

The basic assumptions of the analysis are as follows:

1. The motion of the wing is restricted to a single degree of freedom, namely, torsion.

2. The flutter frequency $\omega$ is assumed to be equal to the natural torsional frequency $\omega_\alpha$.

If the approach used in reference 11 is followed, the total moment contributed by an element of length $dx$ is

$$M = I_\alpha \ddot{\alpha} + C_\alpha(1 + ig_\alpha)\alpha + M_a\alpha \tag{1}$$

where $M_a$ is the complex aerodynamic moment per unit span per radian deflection.

The time rate of change of energy of each of the elements is equal to its total moment multiplied by its angular velocity. The rate of change of total energy for the entire wing having only torsional motion is simply the sum of the energy rates contributed by each of the elements

$$\frac{dE}{dt} = \int_0^L M\dot{\alpha}\, dx \tag{2}$$

At the flutter condition the time rate of change of energy must equal zero. Substituting the expression for the moment, equation (1), into the expression for energy, equation (2), and setting the total rate of change of energy equal to zero produces

$$\frac{dE}{dt} = \int_0^L \left[I_\alpha \ddot{\alpha} + C_\alpha(1 + ig_\alpha)\alpha + M_a\alpha\right]\dot{\alpha}\, dx = 0 \tag{3}$$

The motion of each element is harmonic and can be expressed as

$$\alpha = \alpha_o \left[f_\alpha(x)\right] e^{i\omega t}$$

where $f_\alpha(x)$ represents the spanwise mode shape for torsional vibrations. It is assumed that the aerodynamic terms do not appreciably change the mode shape.

If this relation is used and $C_\alpha = I_\alpha \omega_\alpha^2$ is defined, equation (3) becomes

$$\left[-\omega^2 + \omega_\alpha^2(1 + ig_\alpha)\right] \int_0^L I_\alpha \left[f_\alpha(x)\right]^2 dx + \int_0^L M_a \left[f_\alpha(x)\right]^2 dx = 0 \qquad (4)$$

Equation (4) can be separated into a real and an imaginary equation both of which must vanish to provide a solution to (4). Since it has been observed that in most cases of stall flutter $\omega \cong \omega_\alpha$, the real part of equation (4) must approach zero. Normally the real part of equation (4) is used to provide the flutter frequency but, since the flutter frequency has been assumed to be equal to the natural torsional frequency, the solution of the real part of equation (4) will not be required.

The imaginary part of equation (4), solutions of which provide the flutter velocity, is

$$\omega_\alpha^2 g_\alpha \int_0^L I_\alpha \left[f_\alpha(x)\right]^2 dx + \int_0^L (\text{imag.}) M_a \left[f_\alpha(x)\right]^2 dx = 0 \qquad (5)$$

or

$$\omega_\alpha^2 g_\alpha \int_0^L I_\alpha \left[f_\alpha(x)\right]^2 dx + 2\rho V^2 \int_0^L m_{\dot{\alpha}} b^2 \left[f_\alpha(x)\right]^2 dx = 0 \qquad (6)$$

The first part of equation (6) represents the structural damping energy whereas the second part represents the aerodynamic damping energy. If it is assumed that a representative value of the semichord can be chosen for purposes of defining $V/b\omega_\alpha$, that is, $m_{\dot{\alpha}}$ not a function

of x, then equation (6) can be simplified as

$$g_\alpha \frac{\int_0^L I_\alpha \left[f_\alpha(x)\right]^2 dx}{\int_0^L \pi\rho b^4 \left[f_\alpha(x)\right]^2 dx} + \frac{2m_\alpha'}{\pi}\left(\frac{V}{b\omega_\alpha}\right)^2 = 0$$

or

$$g_\alpha \left(\frac{r_\alpha^2}{\kappa}\right)_e + \frac{2m_\alpha'}{\pi}\left(\frac{V}{b\omega_\alpha}\right)^2 = 0 \tag{7}$$

where $\left(\frac{r_\alpha^2}{\kappa}\right)_e$ represents the effective or mean value of the important inertia parameter $\frac{r_\alpha^2}{\kappa}$.

## REFERENCES

1. Frazer, R. A., and Duncan, W. J.: The Flutter of Aeroplane Wings. R. & M. No. 1155, British A.R.C., 1928.

2. Studer, Hans-Luzi: Experimentelle Untersuchungen über Flügelschwingungen. Mitt. no. 4, Inst. für Aerod. Tech. H. S. Zürich, Gebr. Leemann & Co. (Zürich), 1936.

3. Rauscher, Manfred: Model Experiments on Flutter at the Massachusetts Institute of Technology. Jour. Aero. Sci., vol. 3, no. 5, March 1936, pp. 171-172.

4. Bollay, William, and Brown, Charles D.: Some Experimental Results on Wing Flutter. Jour. Aero. Sci., vol. 8, no. 8, June 1941, pp. 313-318.

5. Victory, Mary: Flutter at High Incidence. R. & M. No. 2048, British A.R.C., 1943.

6. Halfman, Robert L., Johnson, H. C. and Haley, S. M.: Evaluation of High-Angle-of-Attack Aerodynamic-Derivative Data and Stall-Flutter Prediction Techniques. NACA TN 2533, 1951.

7. Baker, John E.: The Effects of Various Parameters, Including Mach Number, on Propeller-Blade Flutter With Emphasis on Stall Flutter. NACA TN 3357, 1955. (Supersedes NACA RM L50L12b.)

8. Bratt, J. B., Wight, K. C., and Chinneck, A.: Free Oscillations of an Aerofoil About the Half-Chord Axis at High Incidences, and Pitching Moment Derivatives for Decaying Oscillations. R. & M. No. 2214, British A.R.C., 1940.

9. Myklestad, N. O.: Vibration Analysis. McGraw-Hill Book Co., Inc., 1944, pp. 161-162.

10. McCullough, George B., and Gault, Donald E.: Examples of Three Representative Types of Airfoil-Section Stall at Low Speed. NACA TN 2502, 1951.

11. Smilg, Benjamin, and Wasserman, Lee S.: Application of Three-Dimensional Flutter Theory to Aircraft Structures. ACTR No. 4798, Materiel Div., Army Air Corps, July 9, 1942.

TABLE I

MODEL PARAMETERS AND CONDITIONS AT THE MINIMUM FLUTTER VELOCITY

| Model designation | Aspect ratio | $\Lambda$ (deg) | $f_{h_1}$ (cps) | $f_{\alpha_1}$ (cps) | $g_\alpha$ | b (ft) | $\alpha_1$ (deg) | V (ft/sec) | $V/b\omega_\alpha$ | Mach number | $R \times 10^{-6}$ | a (ft/sec) | $b\omega_\alpha/a$ | Percent Freon | Density $\rho$ (slug/cu ft) | $f_{exp}$ (cps) | Test section (ft) |
|---|---|---|---|---|---|---|---|---|---|---|---|---|---|---|---|---|---|
| 1-24 | 6.0 | 0 | 17.3 | 102.3 | 0.0010 | 0.333 | 20 | 171.8 | 0.803 | 0.149 | 0.651 | 1152.8 | 0.186 | 0 | 0.00222 | 100.2 | 4.5 diam. |
| 1-24 | 6.0 | 0 | 17.3 | 102.3 | .0010 | .333 | 22 | 173.5 | .811 | .151 | .332 | 1149.1 | .186 | 0 | .00112 | 102.2 | 4.5 diam. |
| 1-24 | 6.0 | 0 | 17.3 | 102.3 | .0010 | .333 | 20 | 178.1 | .832 | .154 | .162 | 1157.9 | .185 | 0 | .00054 | 103.0 | 4.5 diam. |
| 1-24 | 6.0 | 0 | 17.3 | 102.3 | .0010 | .333 | 20 | 181.1 | .846 | .160 | .085 | 1135.5 | .189 | 0 | .00027 | 103.0 | 4.5 diam. |
| 1-24 | 6.0 | 0 | 17.3 | 102.3 | .0010 | .333 | 20 | 160.6 | .750 | .322 | 3.411 | 499.0 | .429 | 97.0 | .00846 | 92.1 | 4.5 diam. |
| 1-24 | 6.0 | 0 | 17.3 | 102.3 | .0010 | .333 | 20 | 170.5 | .796 | .336 | 1.853 | 507.8 | .422 | 94.8 | .00441 | 97.4 | 4.5 diam. |
| 1-24 | 6.0 | 0 | 17.3 | 102.3 | .0010 | .333 | 20 | 182.6 | .853 | .344 | .849 | 531.0 | .403 | 87.1 | .00198 | 100.9 | 4.5 diam. |
| 1-24 | 6.0 | 0 | 17.3 | 102.3 | .0010 | .333 | 20 | 188.4 | .880 | .326 | .346 | 578.0 | .370 | 69.3 | .00083 | ----- | 4.5 diam. |
| 1-21 | 5.25 | 0 | 22.0 | 121.4 | .0010 | .333 | 20 | 217.3 | .855 | .215 | .137 | 1010.0 | .252 | 6.7 | .00035 | 120.0 | 2 × 4 |
| 1-21 | 5.25 | 0 | 22.0 | 121.4 | .0010 | .333 | 19 | 272.3 | 1.071 | .537 | 5.341 | 507.0 | .502 | 93.9 | .00781 | 115.8 | 2 × 4 |
| 1-21 | 5.25 | 0 | 22.0 | 121.4 | .0010 | .333 | 18.5 | 291.1 | 1.145 | .568 | 2.846 | 513.0 | .496 | 90.7 | .00395 | 116.7 | 2 × 4 |
| 1-21 | 5.25 | 0 | 22.0 | 121.4 | .0010 | .333 | 20 | 217.3 | .855 | .392 | .911 | 555.0 | .458 | 81.1 | .00184 | 120.7 | 2 × 4 |
| 1-21W | 5.25 | 0 | ---- | 68.0 | .0057 | .333 | 9.5 | 358.1 | 2.513 | .324 | .204 | 1107.0 | .128 | 2.2 | .00032 | 67.7 | 2 × 4 |
| 1-18 | 4.5 | 0 | 29.2 | 143.7 | .0012 | .333 | 18 | 287.9 | .956 | .251 | .120 | 1147.0 | .262 | 0 | .00024 | 143.7 | 2 × 4 |
| 1-18 | 4.5 | 0 | 29.2 | 143.7 | .0012 | .333 | 18.3 | 299.6 | .996 | .600 | 2.926 | 514.5 | .585 | 92.3 | .00385 | 140.0 | 2 × 4 |
| 1-18 | 4.5 | 0 | 29.2 | 143.7 | .0012 | .333 | 18.3 | 290.0 | .964 | .561 | 2.611 | 517.0 | .582 | 91.6 | .00365 | 140.0 | 2 × 4 |
| 1-18 | 4.5 | 0 | 29.2 | 143.7 | .0012 | .333 | 18.3 | 287.3 | .955 | .538 | 1.114 | 534.0 | .564 | 85.2 | .00163 | 145.0 | 2 × 4 |
| 1-18 | 4.5 | 0 | 29.2 | 143.7 | .0012 | .333 | 20.2 | 268.9 | .894 | .481 | .916 | 559.0 | .538 | 76.5 | .00149 | 145.0 | 2 × 4 |
| 1-18W | 4.5 | 0 | 17.4 | 81.9 | .0052 | .333 | 8.0 | 568.5 | 3.275 | .500 | .269 | 1137.0 | .151 | 0 | .00027 | 81.3 | 2 × 4 |
| 1-18W | 4.5 | 0 | 17.4 | 81.9 | .0052 | .333 | 14.0 | 262.3 | 1.510 | .476 | .102 | 551.0 | .311 | 78.5 | .00172 | 81.3 | 2 × 4 |
| 1-15 | 3.75 | 0 | 41.1 | 179.1 | .001 | .333 | 18.3 | 391.7 | 1.043 | .697 | 1.420 | 562.0 | .668 | 77.9 | .00147 | 175.0 | 2 × 4 |
| 1-15 | 3.75 | 0 | 41.1 | 179.1 | .001 | .333 | 18.3 | 427.2 | 1.139 | .794 | 1.308 | 538.0 | .698 | 85.2 | .00142 | 175.0 | 2 × 4 |
| 2 | 5.4 | 0 | 10.1 | 36.2 | .017 | .208 | 16.0 | 48.0 | .973 | .042 | .116 | 1146.0 | .041 | 0 | .00226 | 35.7 | 4.5 diam. |
| 2 | 5.4 | 0 | 10.1 | 36.2 | .017 | .208 | 14.0 | 56.0 | 1.184 | .049 | .068 | 1147.0 | .041 | 0 | .00113 | 35.2 | 4.5 diam. |
| 2 | 5.4 | 0 | 10.1 | 36.2 | .017 | .208 | 8.0 | 109.9 | 2.322 | .097 | .073 | 1131.0 | .042 | 0 | .00060 | 35.4 | 4.5 diam. |
| 3 | 5.04 | 15 | 10.0 | 40.3 | .02 | .208 | 18.0 | 51.1 | .967 | .045 | .134 | 1134.0 | .047 | 0 | .00231 | 37.8 | 4.5 diam. |
| 3 | 5.04 | 15 | 10.0 | 40.3 | .02 | .208 | 14.0 | 54.1 | 1.025 | .048 | .070 | 1125.0 | .047 | 0 | .00114 | 37.9 | 4.5 diam. |
| 3 | 5.04 | 15 | 10.0 | 40.3 | .02 | .208 | 14.0 | 73.2 | 1.388 | .065 | .049 | 1129.0 | .047 | 0 | .00058 | 38.9 | 4.5 diam. |
| 4 | 4.05 | 30 | 10.6 | 38.1 | .02 | .208 | 20.0 | 58.7 | 1.177 | .052 | .173 | 1132.0 | .044 | 0 | .00233 | ----- | 4.5 diam. |
| 4 | 4.05 | 30 | 10.6 | 38.1 | .02 | .208 | 16.0 | 70.9 | 1.423 | .062 | .099 | 1139.0 | .044 | 0 | .00117 | ----- | 4.5 diam. |
| 4 | 4.05 | 30 | 10.6 | 38.1 | .02 | .208 | 8.0 | 203.2 | 4.079 | .179 | .152 | 1136.0 | .044 | 0 | .00059 | 38.8 | 4.5 diam. |
| 5 | 2.7 | 45 | 12.4 | 40.9 | .02 | .208 | 8.0 | 354.3 | 6.616 | .311 | 1.160 | 1141 | .047 | 0 | .00217 | ----- | 4.5 diam. |

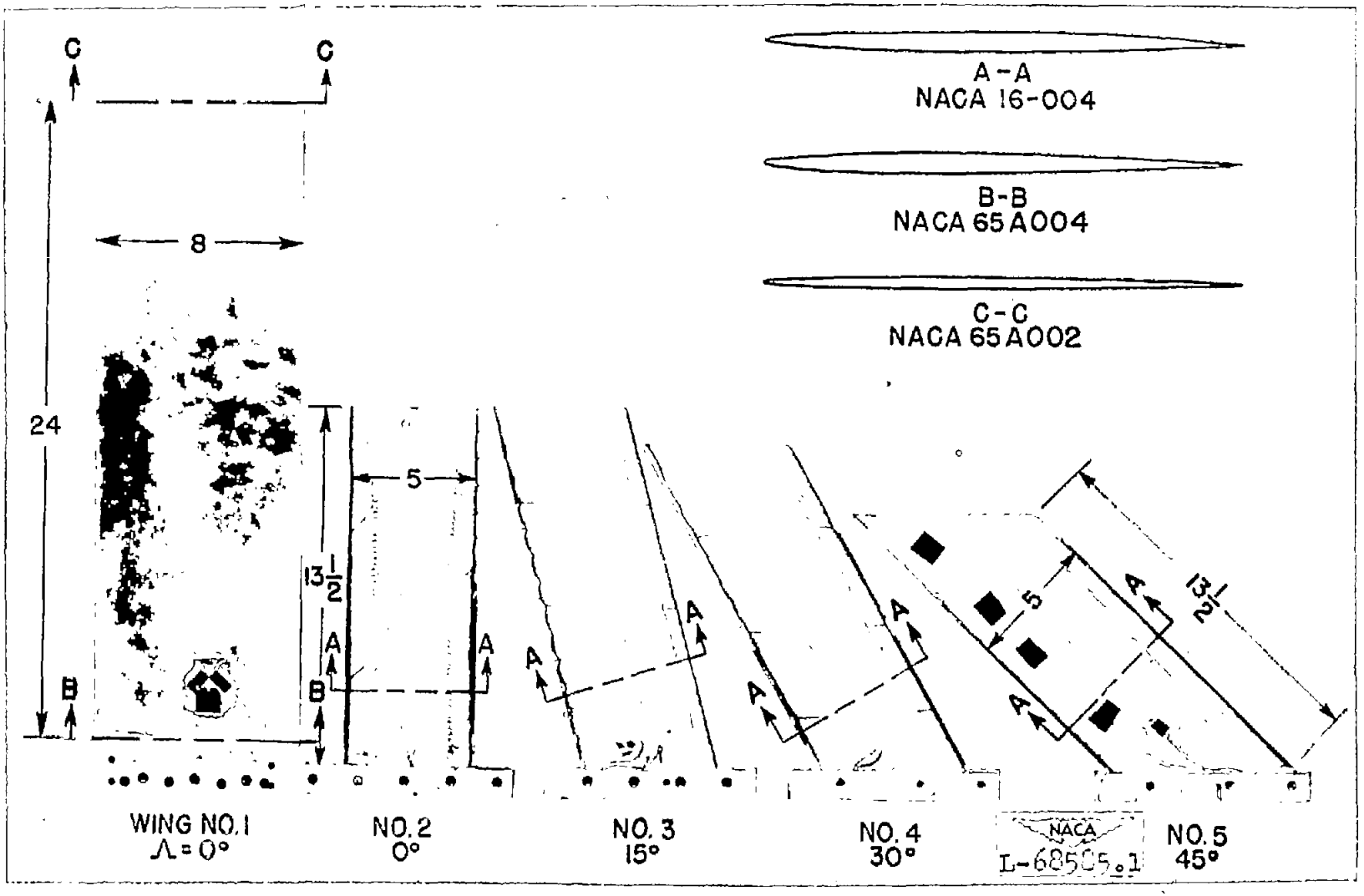


Figure 1.- Flutter models.

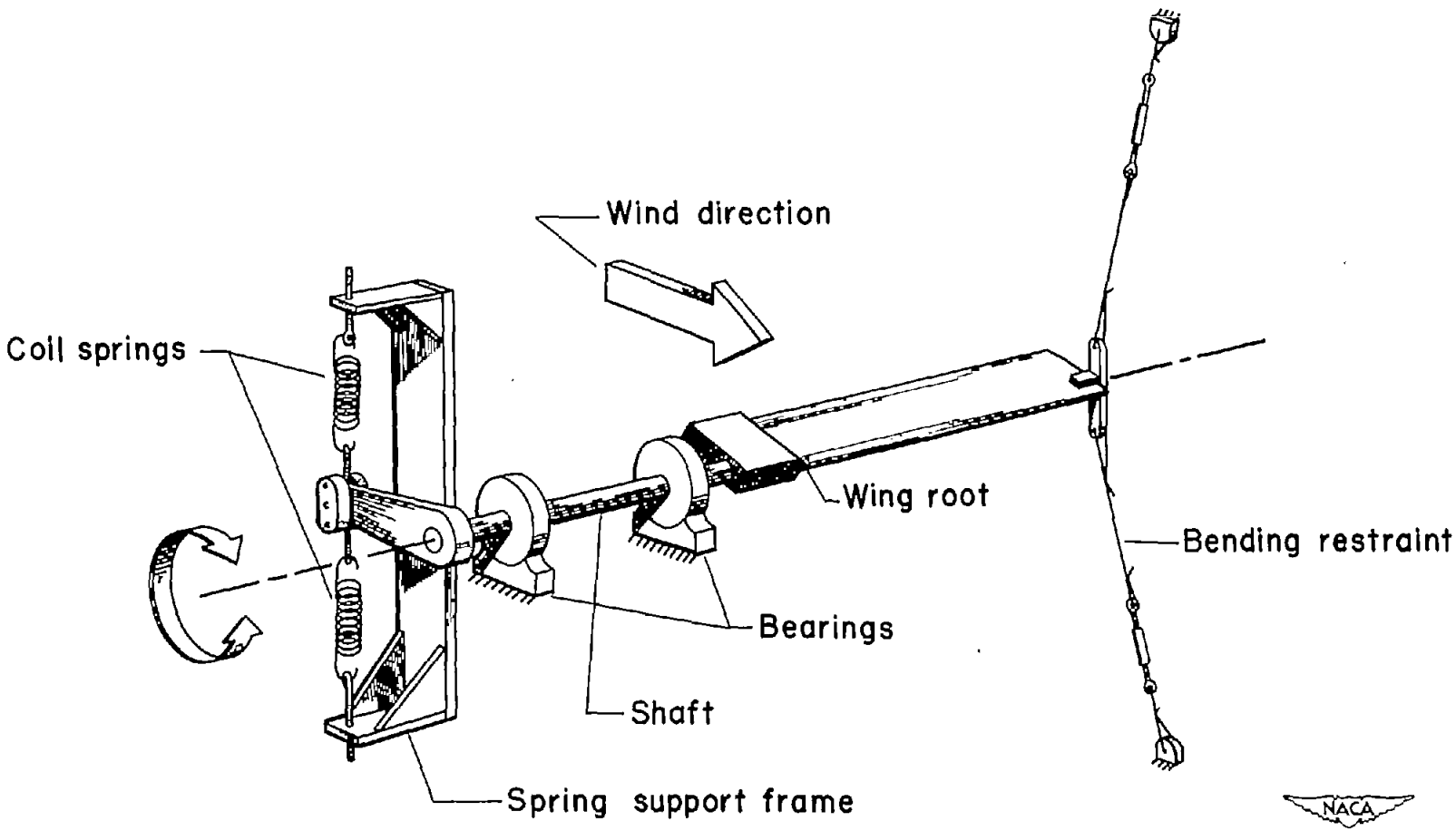


Figure 2.- Aerodynamic damping mechanism.

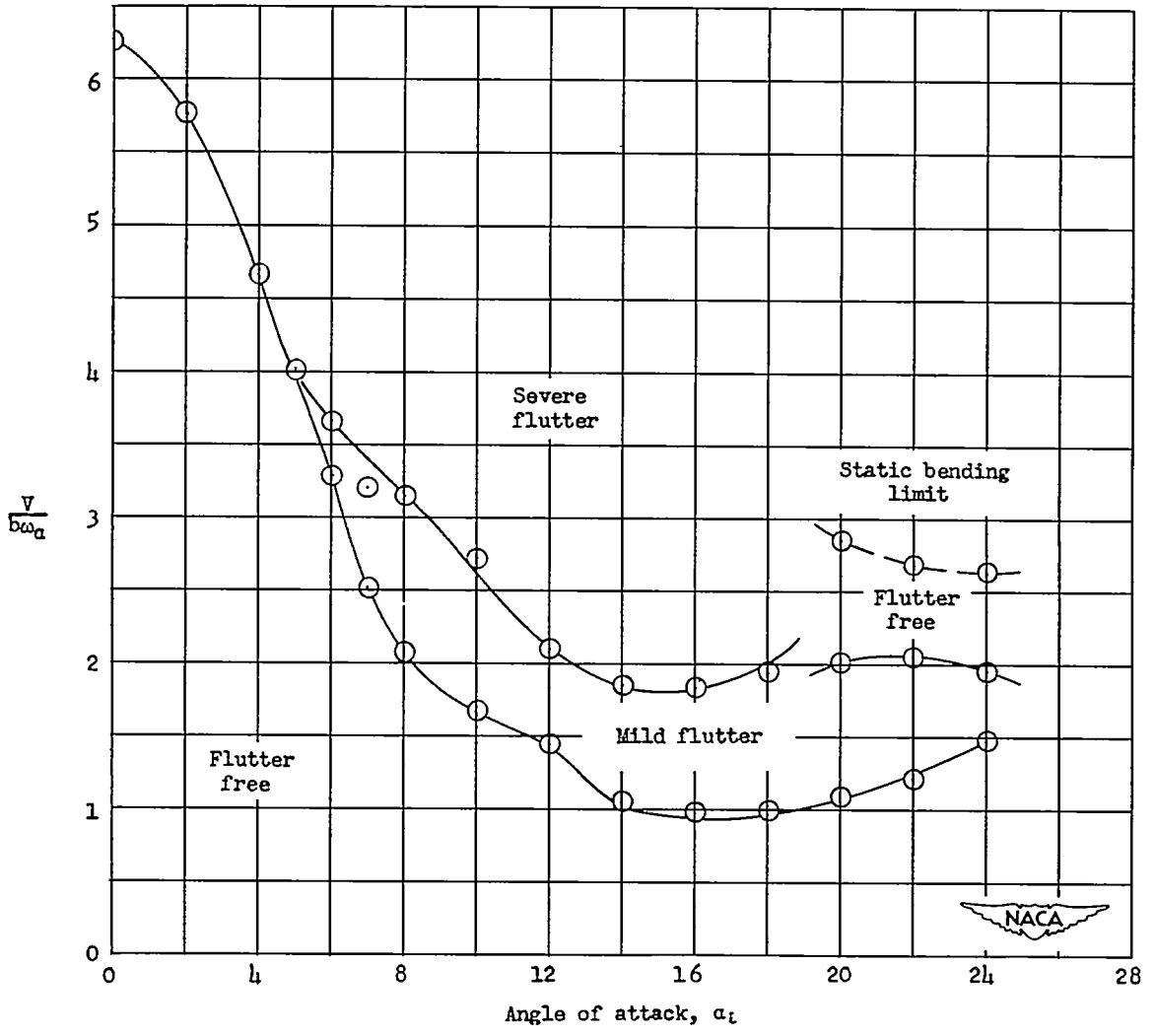


Figure 3.- Flutter regions for wing number 2 at one atmosphere in air.

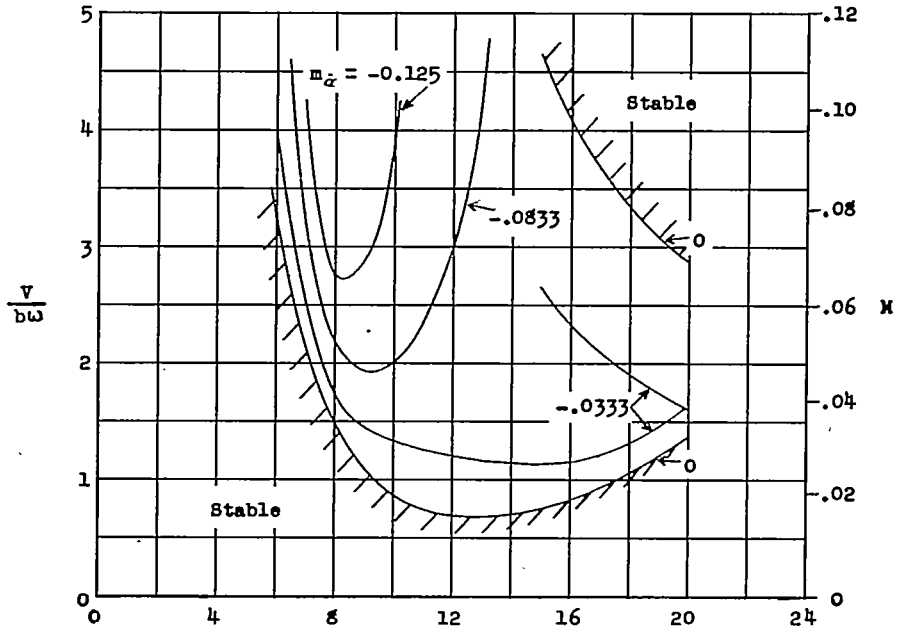


(a) Contours of constant aerodynamic torsional damping coefficient as functions of $V/b\omega$ and $\alpha_1$. Axis of rotation at 0.50c.

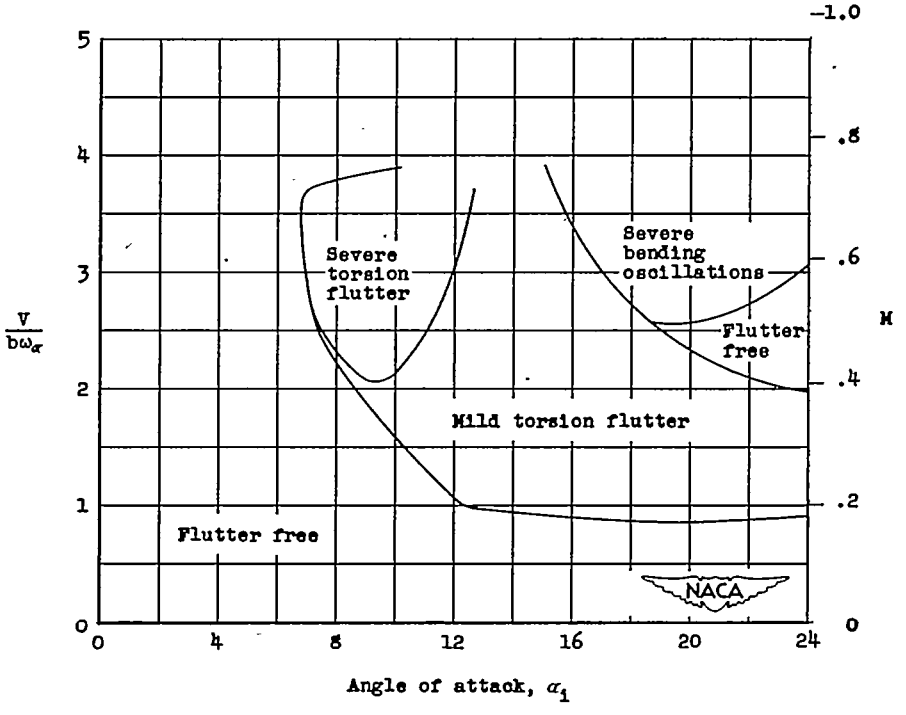


(b) Flutter regions for wing number 1-24 at 1/8 atmosphere in air.

Figure 4.- Comparison of flutter regions and damping contours.

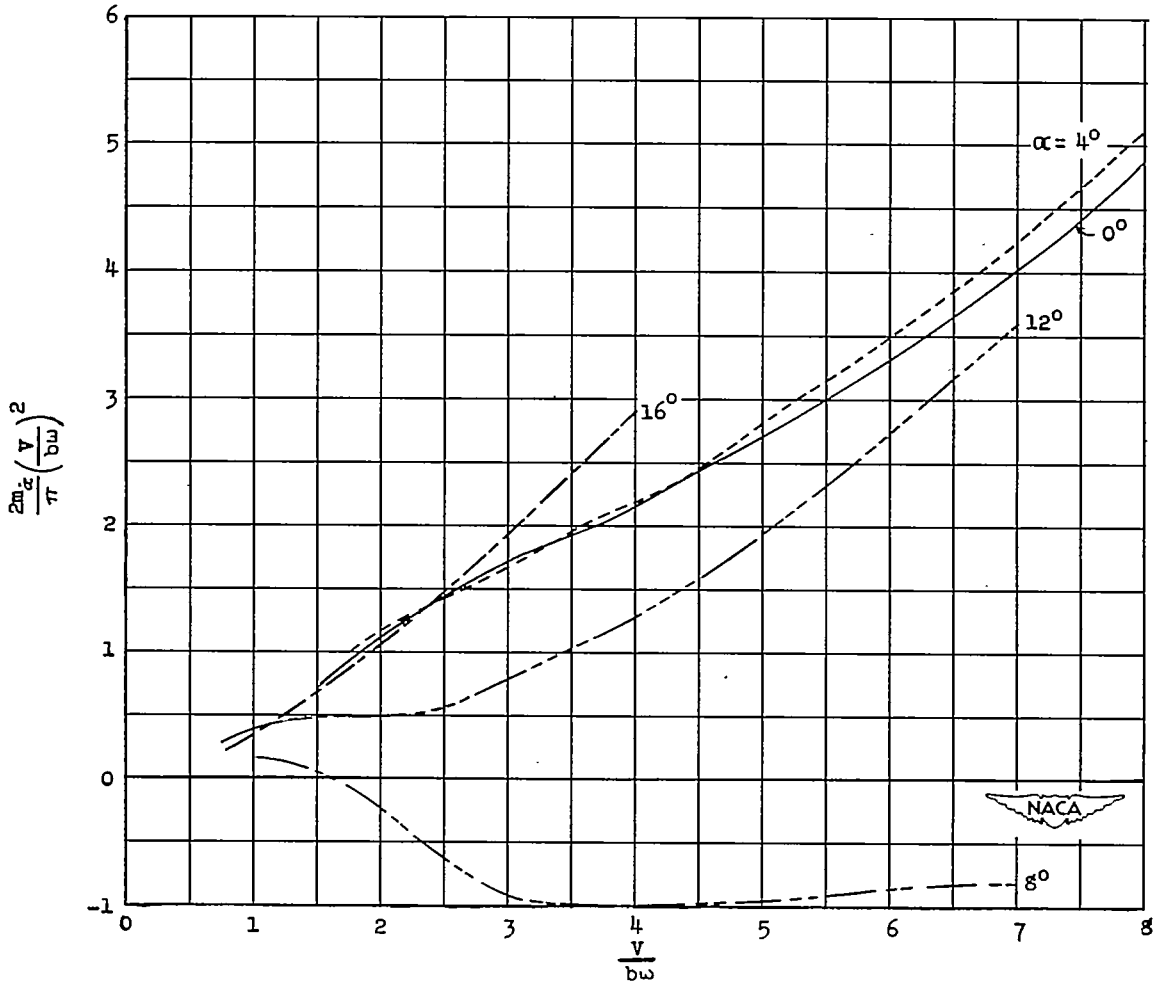


(a) Axis of rotation at 0.25c.

Figure 5.- Variation of $\frac{2m_{\dot{\alpha}}}{\pi}\left(\frac{V}{b\omega}\right)^2$ with $\frac{V}{b\omega}$ for various angles of attack.

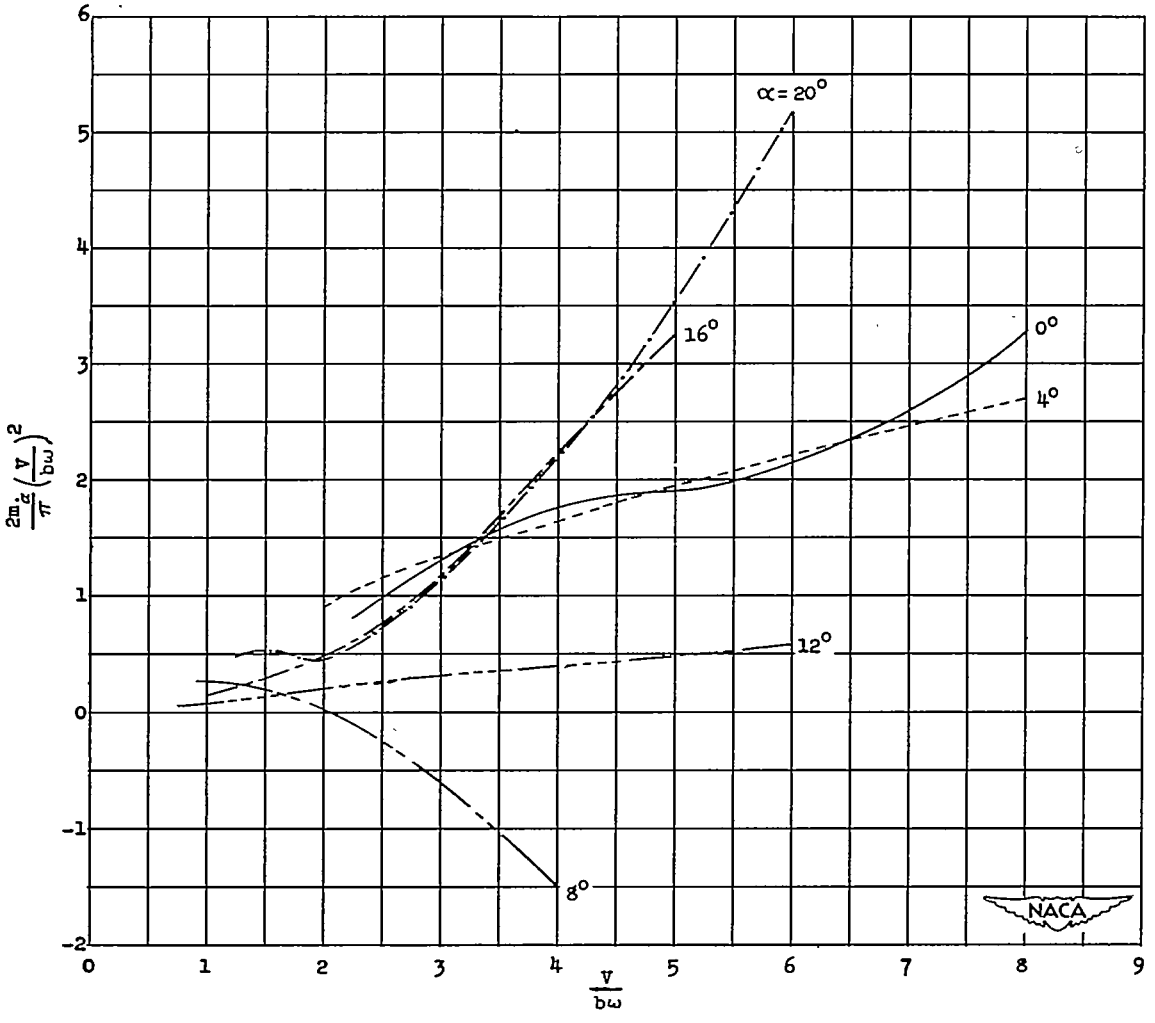


(b) Axis of rotation at 0.325c.

Figure 5.- Continued.

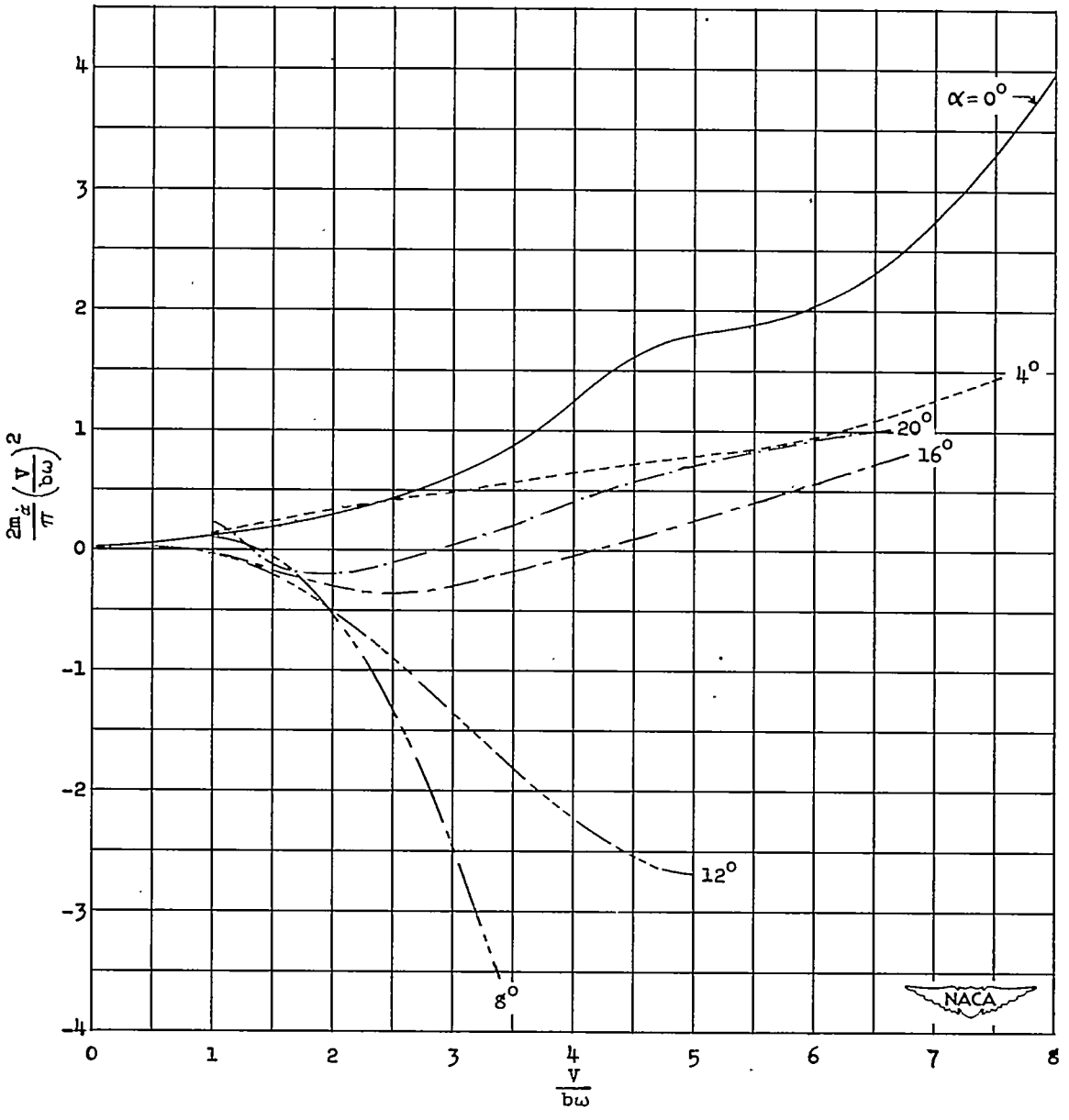


(c) Axis of rotation at 0.50c.

Figure 5.- Continued.

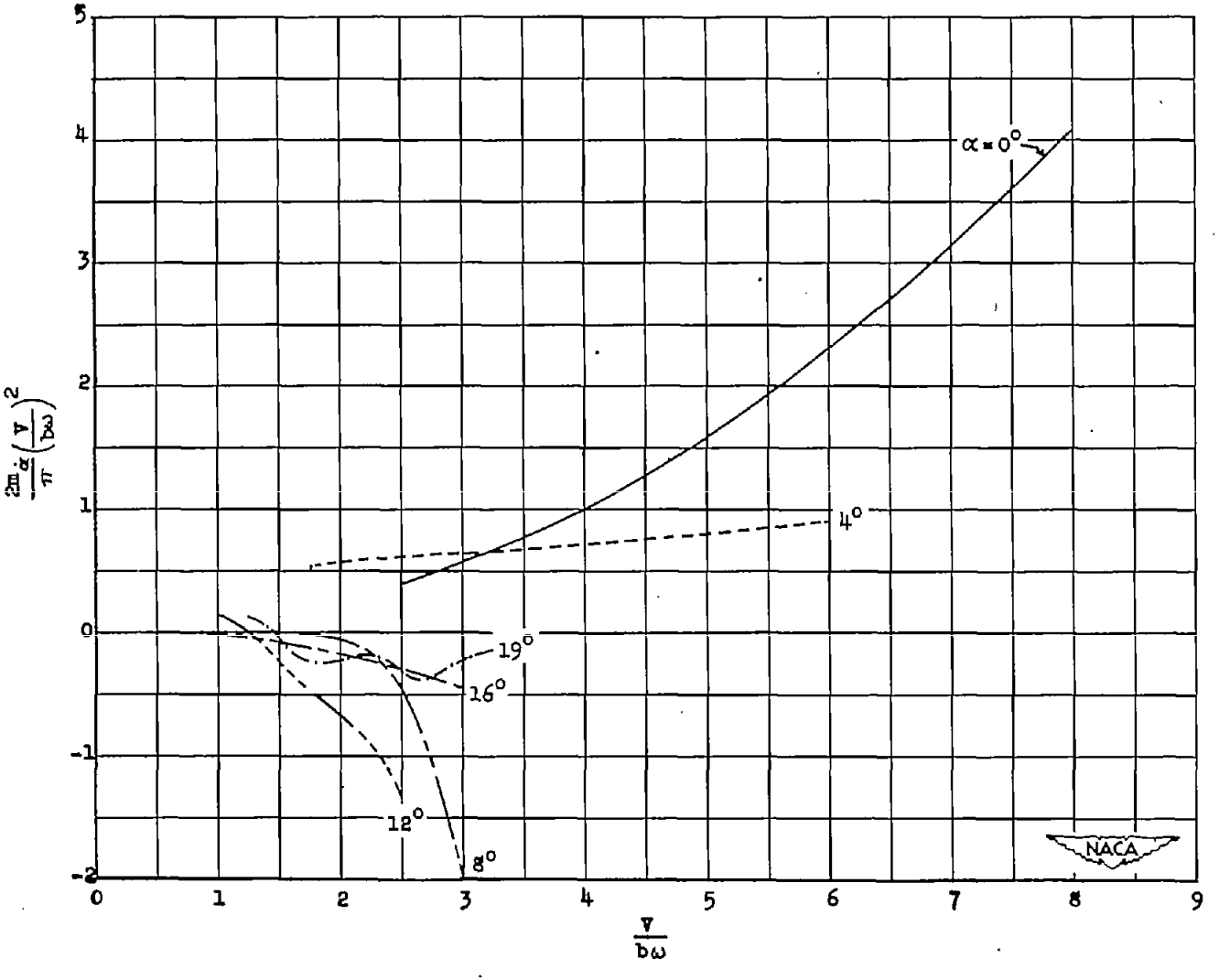


(d) Axis of rotation at 0.75c.

Figure 5.- Concluded.

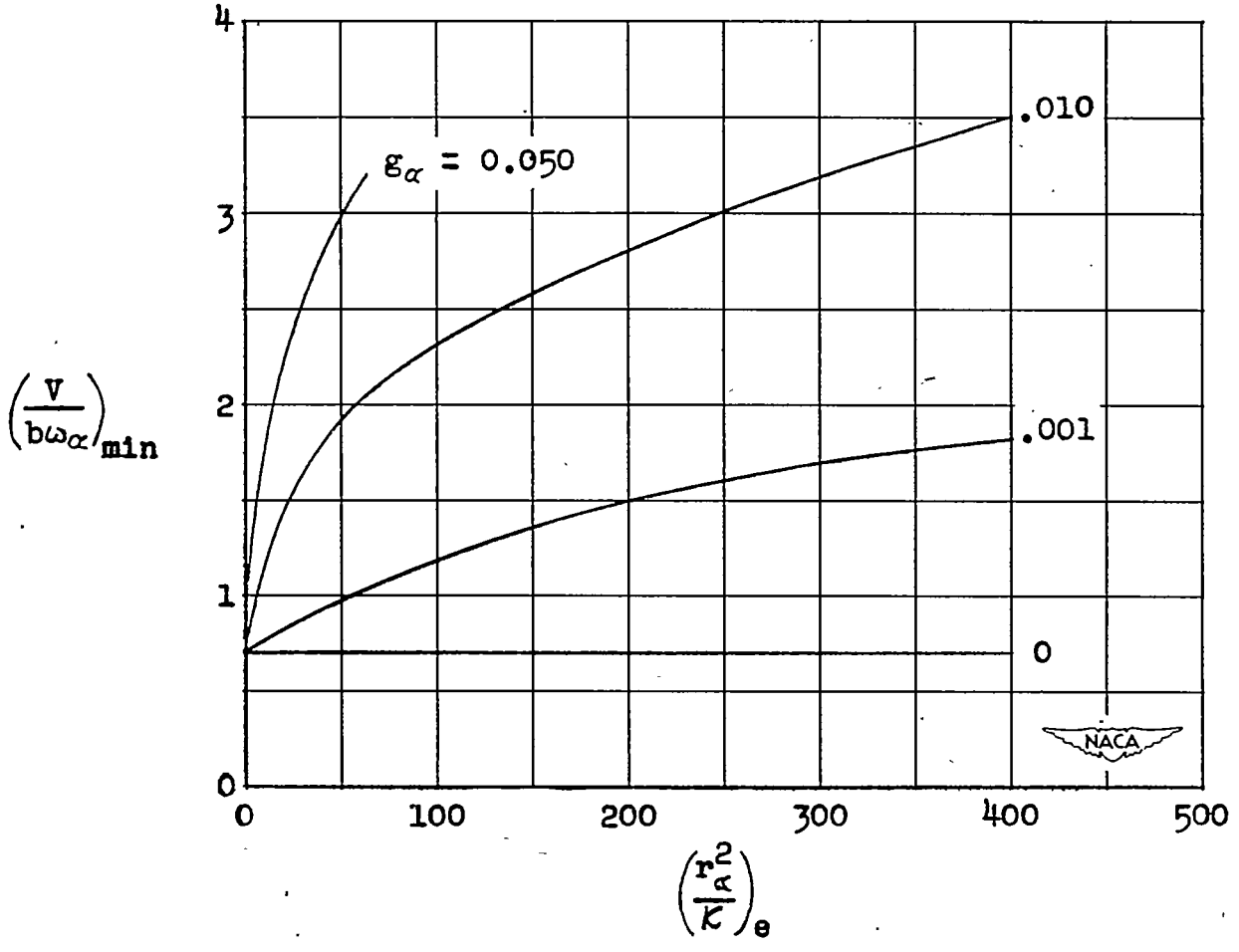


Figure 6.- Calculated variation of minimum flutter velocity coefficient with effective inertia parameter for various values of structural damping. Axis of rotation at 0.5c.

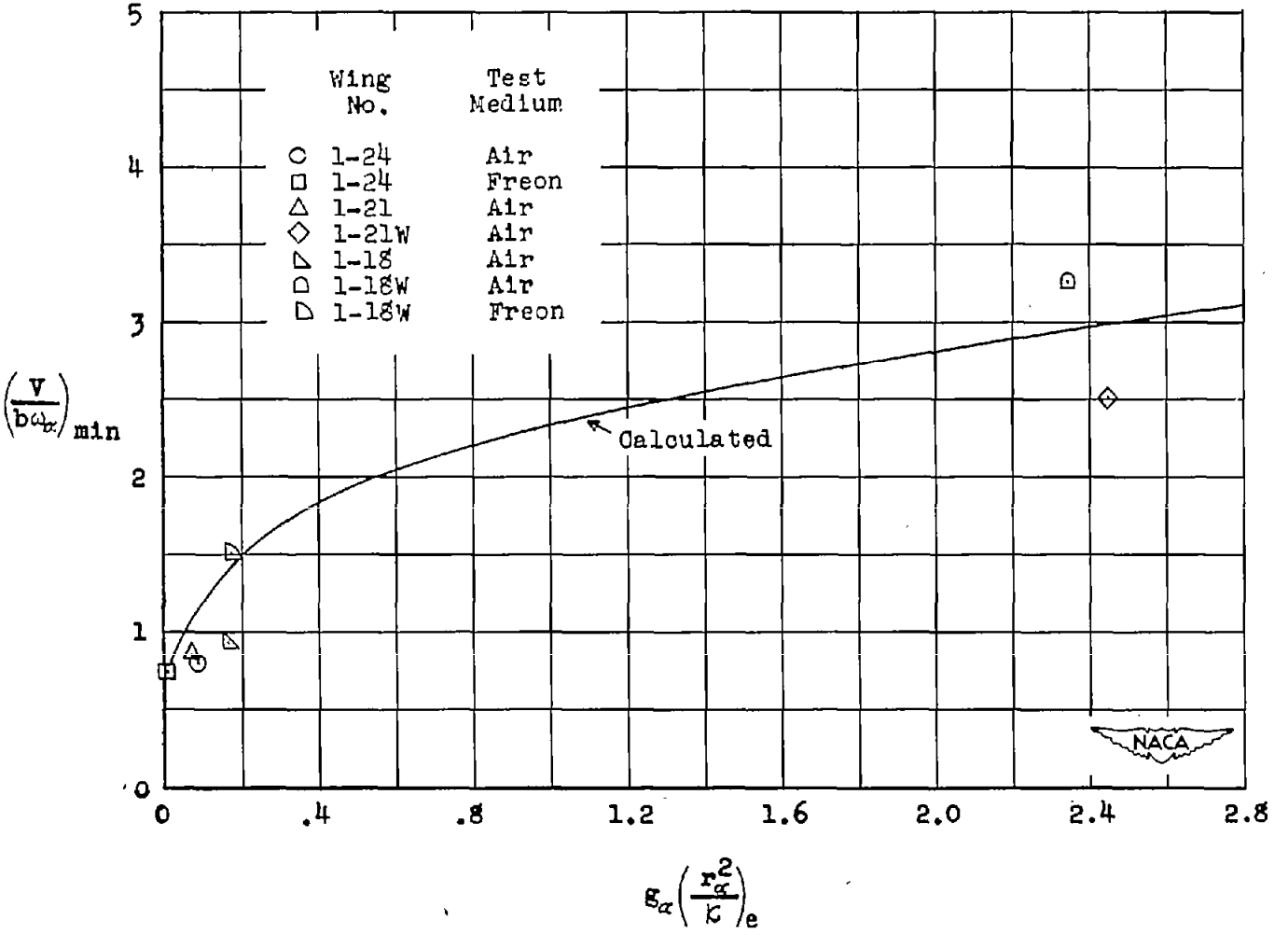


Figure 7.- Comparison of experimental and calculated minimum flutter velocity coefficients for wings number 1-24 to 1-18 at various densities with and without a concentrated tip weight.

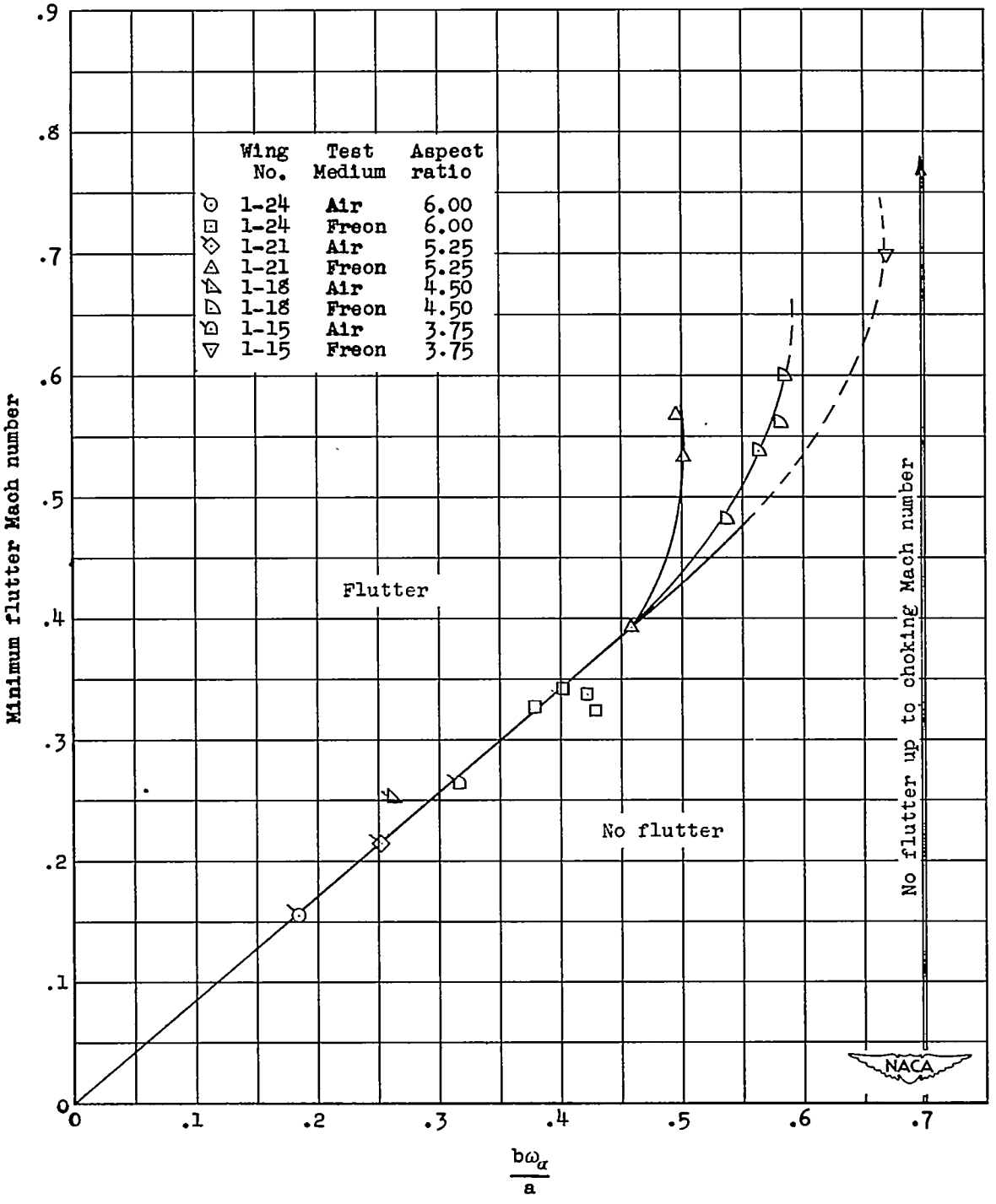


Figure 8.- Variation of minimum flutter Mach number with $\frac{b\omega_\alpha}{a}$.

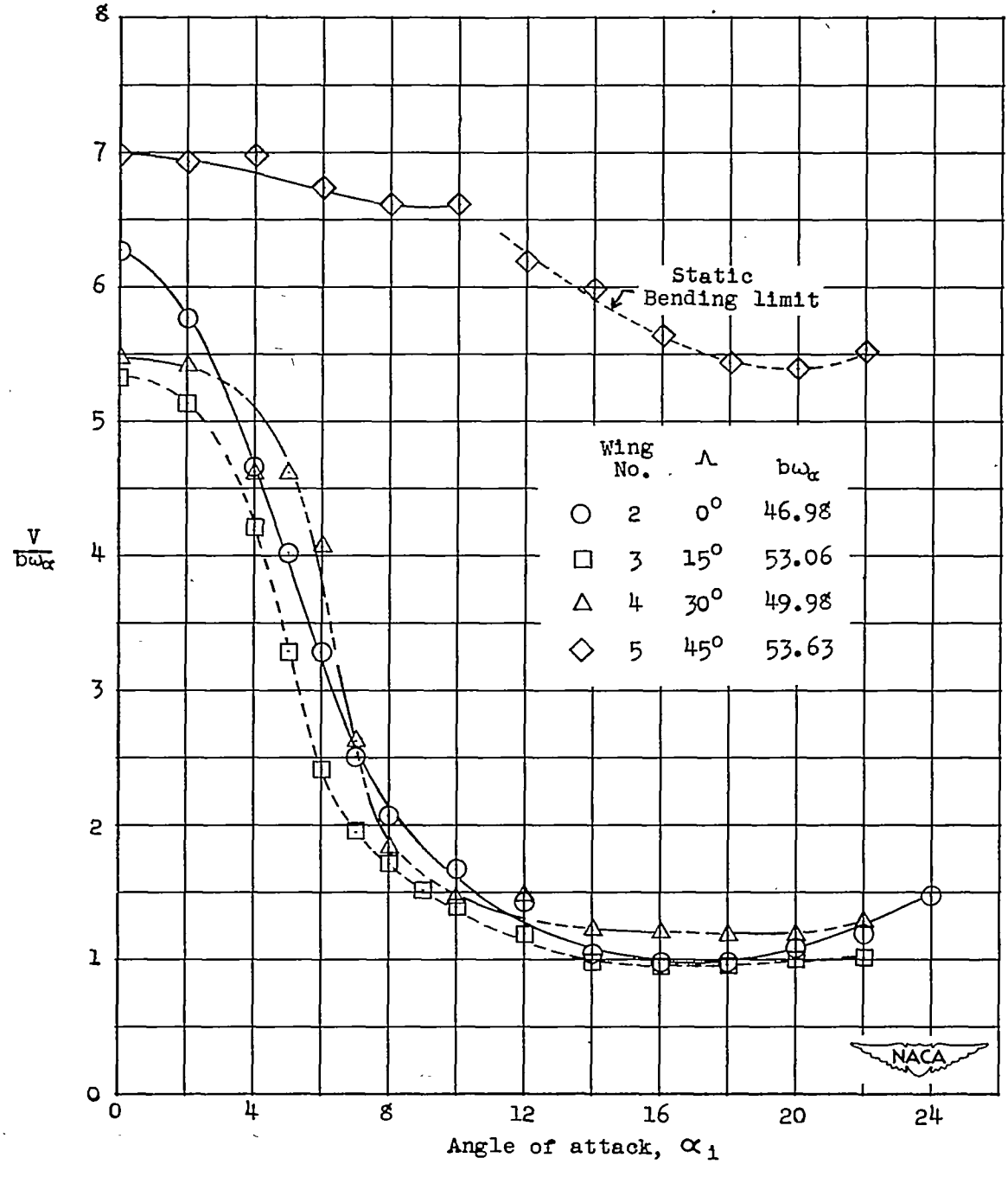


Figure 9.- Variation of flutter velocity coefficient with angle of attack for various angles of sweepback at 1 atmosphere in air.

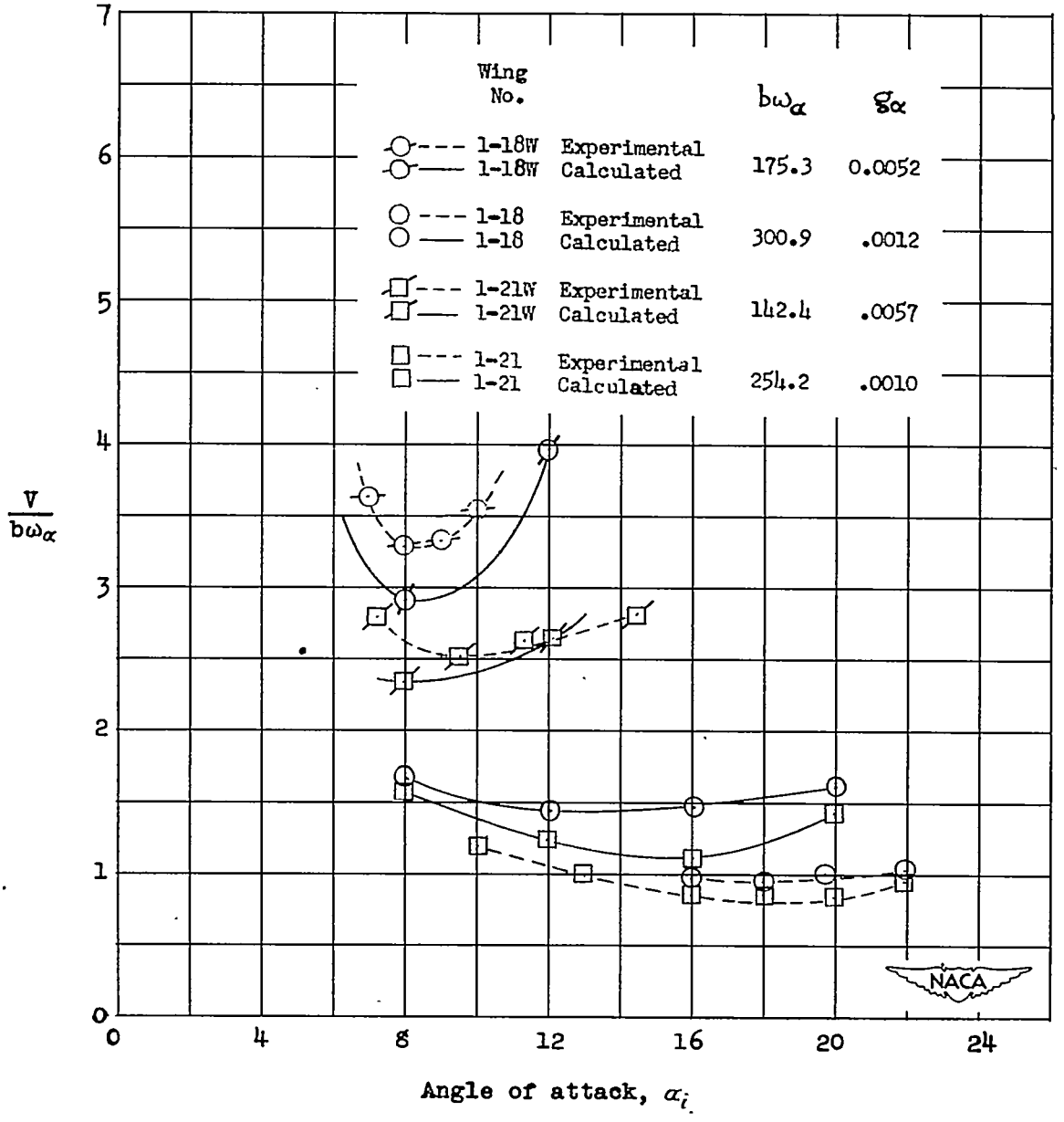


Figure 10.- Comparison of experimental and calculated flutter velocity coefficients for wings number 1-21 and 1-18 with and without concentrated tip weight at 1/8 atmosphere in air.